論文 / 著書情報
Article / Book Information

Title	Seismic Response Characteristics of long-span domes: Roof-substructure interaction
Authors	D.Nair, B.Sitler, Y.Terazawa, T.Takeuchi
Pub. date	2020, 9
Citation	2020 17WCEE Proceedings

17th World Conference on Earthquake Engineering, 17WCEE
Sendai, Japan - September 13th to 18th 2020

SEISMIC RESPONSE CHARACTERISTICS OF LONG-SPAN DOMES: ROOF-SUBSTRUCTURE INTERACTION

D. Nair[(1)], B. Sitler[(1)], Y. Terazawa[(2)], T. Takeuchi[(3)]

[(1)] *Graduate Student, Tokyo Institute of Technology, nair.d.aa@m.titech.ac.jp, sitler.b.aa@m.titech.ac.jp*
[(2)] *Assistant Professor, Tokyo Institute of Technology, terazawa.y.aa@m.titech.ac.jp*
[(3)] *Professor, Tokyo Institute of Technology, takeuchi.t.ab@m.titech.ac.jp*

Abstract

Seismic response of lattice shell roofs with substructures are known to be complicated as these roofs exhibit various closely spaced modes whose amplitudes are strongly influenced by parameters like rise to span ratio of the dome and ratio of stiffness of the roof to the substructure. Studies of double-layered medium-span domes with single-storey substructures are available wherein a simplified procedure to evaluate the seismic response has been proposed by using amplification factors. However, literature reviews indicate that studies on seismic response of long-span domes or domes with multi-storey substructures are limited. The fundamental periods of long-span spatial structures are longer, however, the higher modes often coincide with the roof's dominant modes resulting in amplified horizontal and vertical accelerations. This paper aims to present a preliminary investigation on the dynamic response characteristics of double-layered 100m span domes supported by multi-storey substructures employing buckling-restrained braced frames. A parametric study was conducted to understand the effects of mass ratio and substructure stiffness on the contribution of the dominant modes of the structure. The roof-substructure interaction was found to be greatly influenced by the relative proximity of the dominant roof and substructure modes which were directly affected by the substructure stiffness and mass ratio. It was concluded that the higher modes of the taller multi-storey substructure and the modes of the long-span roof interact strongly with each other resulting in a significant amplification in the roof response, the effects of which were not accounted for in previous response estimation methods.

Keywords: metal spatial structures; long-span domes; seismic response; roof-substructure interaction; buckling-restrained braces

1. Introduction

The seismic response characteristics of lattice roof systems are known to be complicated owing to a large number of parallel vibration modes. Studies conducted by Ogawa et al. [1] found that medium-span dome roofs with some rise are excited not only in the horizontal direction but also experience large anti-symmetric vertical accelerations when subjected to horizontal earthquake ground motions.

Takeuchi et al. [2] carried out studies to determine the response characteristics of medium-span domes (span~60m) supported by elastic substructures. Amplification factors for roof were proposed to evaluate the seismic response using response spectrum analysis. Subsequently, the inelastic response of a single storey substructure was incorporated to present a simplified procedure to evaluate the seismic response of domes using the prominent anti-symmetric vibration mode of the roofs as shown in Figure 1. The response is evaluated by performing pushover analyses on the dome by applying equivalent static loads. These loads are determined from the maximum seismic accelerations, which may also be of use when designing the acceleration-sensitive non-structural components. Hence, in this paper, the maximum seismic accelerations are chosen as indicators of the seismic response.

2. Analysis Models

Studies conducted by Takeuchi et al. [2] in the past have indicated that double-layered domes exhibit vibration modes that are less varied than the single-layered ones. It was found that for depth-to-span ratios (of the double-layered domes) of 1/50 or more, the response characteristics become simpler and can be explained using the 4 prominent modes which are denoted as O1, O2, O2.5 and I (Fig. 1).

In this study, the roof was modelled as a single-layered dome with a 100m span, and 30° half subtended angle (Fig. 2). The out of plane stiffness of the roof members was increased by a factor of 57 to model an equivalent double-layered dome of a depth-to-span ratio of 1/50. The dome consists of rigidly jointed circular hollow sections (Table 1) and was designed for a uniform 2.44 kPa dead load (DL).

The substructure is chosen so as to represent large-scale sports arenas and stadiums and was designed using Japanese design recommendations limiting the maximum storey drift to within 1% under a level-2 (rare) earthquake [3]. The substructure consists of a moment-resisting frame (MRF) with rigidly jointed beam-column connections enveloping 24 braced frames, spaced equidistantly around the perimeter (Fig. 3). The section sizes are given in Table 1 and the storey weight distribution is given in Table 2. All the frame sections are assigned SN490 (σ_y=325 MPa) material. Each storey is assumed to be 5m high. The braced frames employ energy-dissipating braces called buckling-restrained braces (BRBs) [4] arranged in a diagonal configuration. 24 buckling-restrained braced frames (BRBF) are employed in the circumferential direction of the substructure and each BRBF is placed in between two moment resisting frames (MRF) as shown in Fig. 3. Here, the roof is modelled as a rigid diaphragm. Diagonal braces are added in the top storey to add stiffness in the radial direction to ensure diaphragm action in the combined model.

The BRBs are designed using Kasai's optimal damper distribution method [4] targeting a uniform storey drift throughout the substructure height. Here, it was assumed that at any given time, 12 BRBFs placed around the circumference (along the input direction) are active in resisting the lateral forces. The BRBs are modelled as link elements with parameters as shown in Table 3, and a post-yield stiffness ratio of 2%.

The elevation view at the ridgeline of the combined model (roof plus substructure) is shown in Fig. 4. The connections between the tension ring and both substructure and roof are assumed pinned. The floors are modelled as membrane elements to represent the mass of each floor. These elements essentially transfer the entire loads directly to the structural objects.

This combined model is chosen as the benchmark model in this paper. For the parametric studies to investigate the dynamic response characteristics discussed in the following sections, the BRBs are modelled as elastic braces with stiffness equal to their effective stiffness shown in Table 3.

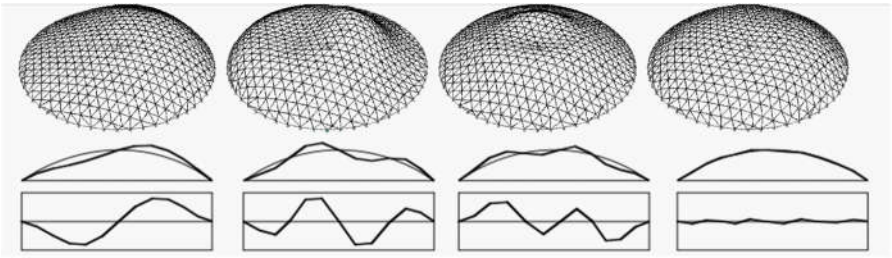

Fig. 1: Four dominant mode shapes of the double-layered dome

Table 1: Frame sections data

Member	Section Type	Size (mm)
Roof	CHS	φ 400 t14.5
Tension Ring	CHS	φ1010 t10
MF Column	SHS	600×600×32
MF Beam	I	450×300×10×16
Elastic Brace	SHS	350×350×16

Table 2: Mass distribution

Storey	Storey Weight (kN)
RFL	20,581
6FL	10,420
5FL	10,420
4FL	19,742
3FL	19,742
2FL	27,968

Table 3: BRB specifications

BRB	δ_y (mm)	k_{eff} (kN/m)
BRB-6FL	5.3	101,373
BRB-5FL	5.3	225,316
BRB-4FL	5.3	318,357
BRB-3FL	5.3	442,784
BRB-2FL	5.3	598,652

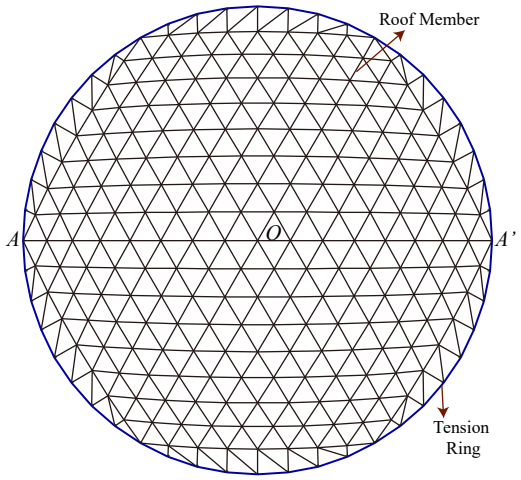

Fig. 2: Plan view of the dome

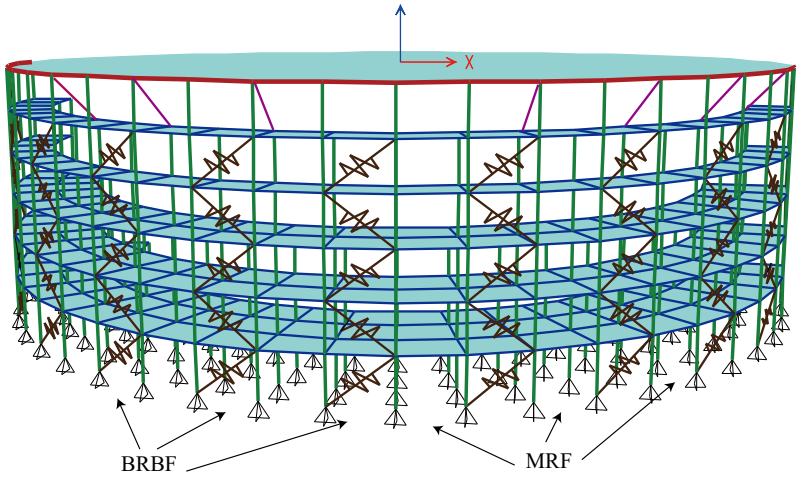

Fig. 3: 3-D view of the substructure model

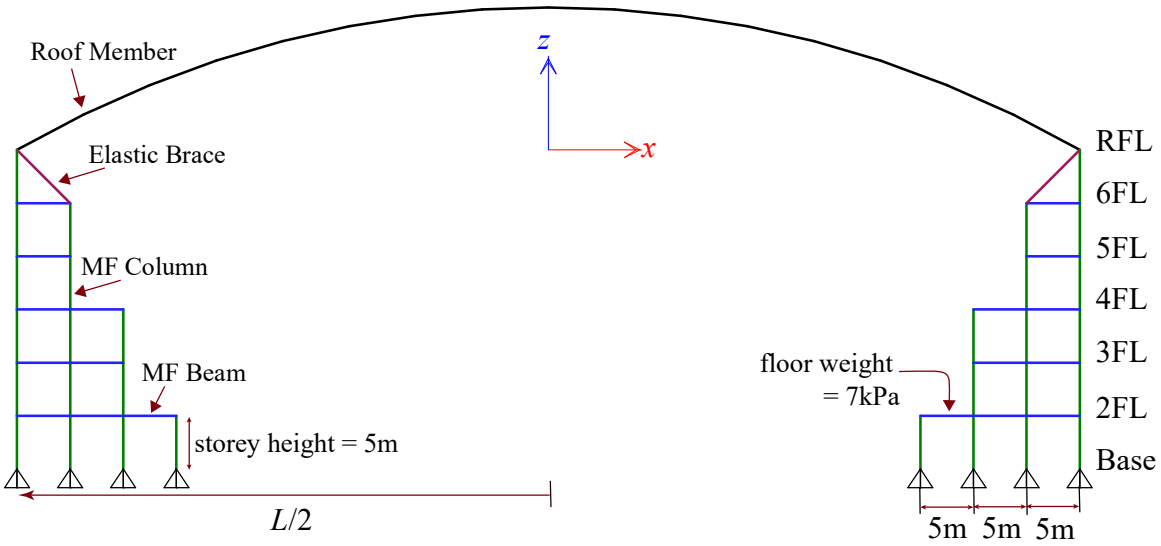

Fig. 4: A-O-A' Elevation view of combined model

3. Effects of Mass Ratio

The response of the roof is known to amplify owing to the roof-substructure interactions. The amplification factors proposed by Takeuchi et al. [2] depend on two main parameters: the total mass to roof mass ratio (R_M) and the period ratio of the fundamental mode of the substructure to the O1 mode of the roof. The effects of R_M on the dynamic response characteristics are investigated in this section.

The dead load on the dome was varied from 1 kPa to 3 kPa as shown in Table 4 and the corresponding periods of the four modes of the roof only model where the roof ends were pinned, and their mass participation factors (β) are summarised in Table 4 and the trends are illustrated in Fig. 5. It can be seen that the periods of the modes generally decreasing with increasing mass ratio as the roof mass is decreasing and so are the periods when the stiffness remains constant. The reduction in the fundamental periods (O1 modes) is the largest whereas the higher mode periods reduce more gradually (Fig. 5a). The mass participation of the O2.5 mode is the highest as the roof ends are pinned and therefore represent a case when the substructure is very rigid. In combined models with substructures of finite stiffness, the fundamental mode, which is the O1 mode in all the roof models, is expected to be the most dominant. Further, it was observed that varying the mass ratios did not change the participation factors of these four periods and the contribution from the individual modes remained rather constant throughout as can be seen in Fig. 5b.

Table 4: Roof Model Periods

Roof Dead Load (kPa)	R_M	O1	O2	O2.5	I
1	11.5	0.25s, (18%)	0.14s, (5%)	0.07s, (57%)	0.05s, (6%)
2	6.2	0.35s, (18%)	0.20s, (5%)	0.11s, (57%)	0.07s, (6%)
3	4.5	0.43s, (18%)	0.24s, (5%)	0.13s, (57%)	0.09s, (6%)

The same exercise was repeated for the substructure model (with the roof modelled as a rigid diaphragm) keeping the mass of the lower floors (2FL-6FL) constant and the results are shown in Table 5 and Fig. 6. Here, the period ratios as R_{T1} and R_{T2} which are the ratios of the first and second substructure period (ranked in decreasing order of mass participation) to the roof's O1 mode period respectively. The effect of mass ratio has a direct correlation to the fundamental periods of the substructure (Fig. 6a), however, the periods of the higher mode period were relatively less affected. As observed in the roof model, varying the mass ratio did not change

the contributions from the individual modes (Fig. 6b). Similarly, varying the mass ratios had a larger influence on R_{T1} which decreased with increasing R_M than on R_{T2} which decreased more gradually.

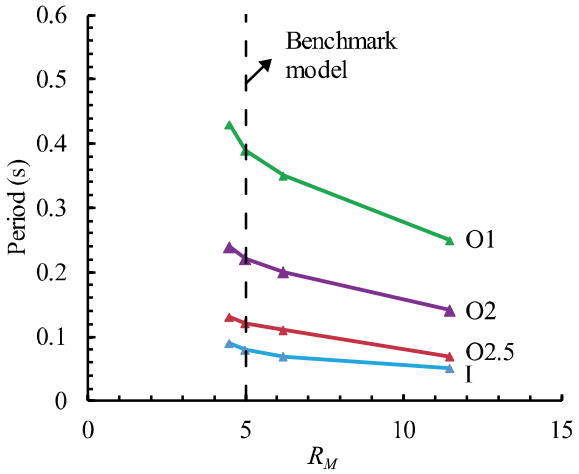

(a) Relationship between roof periods and R_M

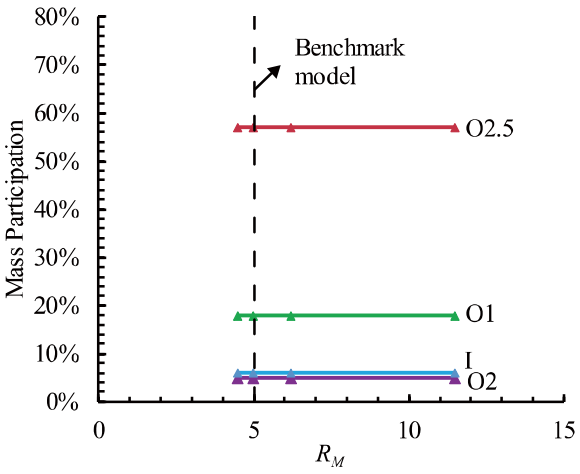

(b) Relationship between mass participation of the four modes and R_M

Fig. 5: Effects of R_M on the dominant modes of the roof model

Table 5: Substructure Model Periods

Roof DL (kPa)	R_M	T_1	T_2	T_3	R_{T1}	R_{T2}
1	11.5	0.57s, (70%)	0.23s, (17%)	0.12s, (6%)	2.28	0.90
2	6.2	0.65s, (68%)	0.25s, (20%)	0.13s, (6%)	1.84	0.70
3	4.5	0.73s, (68%)	0.26s, (21%)	0.14s, (6%)	1.68	0.60

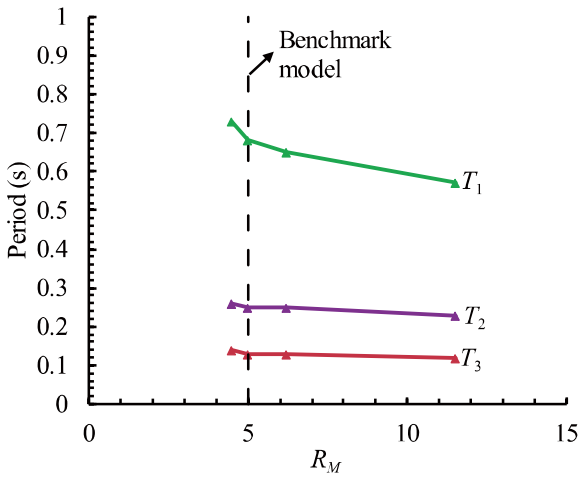

(a) Relationship between substructure periods and R_M

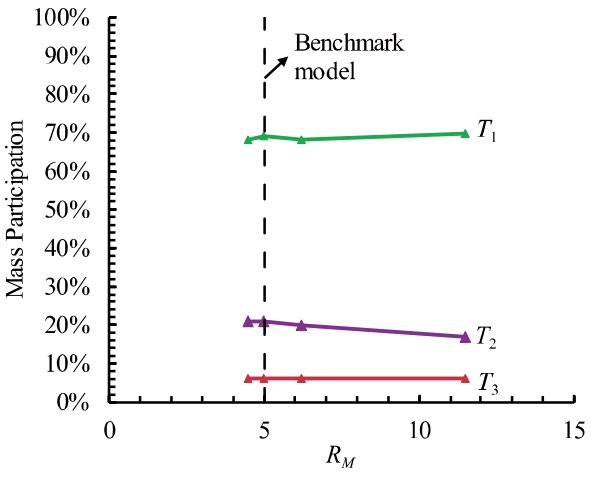

(b) Relationship between mass participation of the top three dominant modes and R_M

Fig. 6: Effects of R_M on the dominant modes of the substructure model

4. Effects of Substructure Stiffness

In this section, the effects of the period ratio as defined in Section 3 is investigated. To study the effects of substructure stiffness, the lateral stiffness of the substructures were increased by multiplying the moment of inertias of MRF members and the axial stiffness of the BRBs by a factor of α. The periods, mode shapes and the mass participation factors of the first three dominant modes of the substructure model are given in Table 6. Increasing the stiffness of the substructures decreased the periods of the dominant modes while also decreasing the participation of the first mode and increasing that of the subsequent higher modes indicating an increase in the contribution from the higher modes. The first three modes are translational modes similar to those observed in a multi-storey building. The first mode participation is around 70% for all the models and the rest of the participation is coming from the higher modes. This implies that the peak acceleration of the substructure (A_{eq}), which is the basis for obtaining the peak roof accelerations [5], cannot be obtained solely from the first modal pushover analysis and the higher mode contributions need to be considered to achieve a minimum cumulative participation factor of 90%.

Table 6: Substructure model periods and mass participation factors

Roof DL (kPa)	R_M	α	T_1(s) and β (%)	T_2(s) and β (%)	T_3(s) and β (%)	R_{T1}	R_{T2}
Mode Shapes			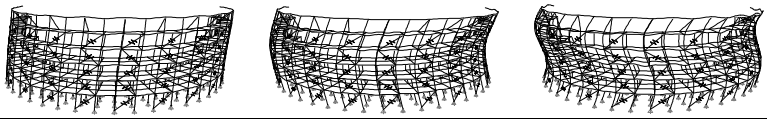				
1	11.5	1/6	1.21s, (72%)	0.50s, (17%)	0.27s, (6%)	4.84	1.99
		1	0.57s, (70%)	0.23s, (17%)	0.12s, (6%)	2.28	0.90
		6	0.34s, (63%)	0.13s, (22%)	0.07s, (6%)	1.34	0.52
2	6.2	1/6	1.35s, (73%)	0.53s, (17%)	0.27s, (6%)	3.82	1.50
		1	0.65s, (68%)	0.25s, (20%)	0.13s, (6%)	1.84	0.70
		6	0.39s, (63%)	0.14s, (22%)	0.07s, (6%)	1.10	0.40
3	4.5	1/6	1.49, (73%)	0.55s, (19%)	0.28s, (6%)	3.45	1.27
		1	0.72s, (68%)	0.26s, (21%)	0.14s, (6%)	1.68	0.60
		6	0.44s, (63%)	0.15s, (21%)	0.07s, (6%)	1.02	0.35

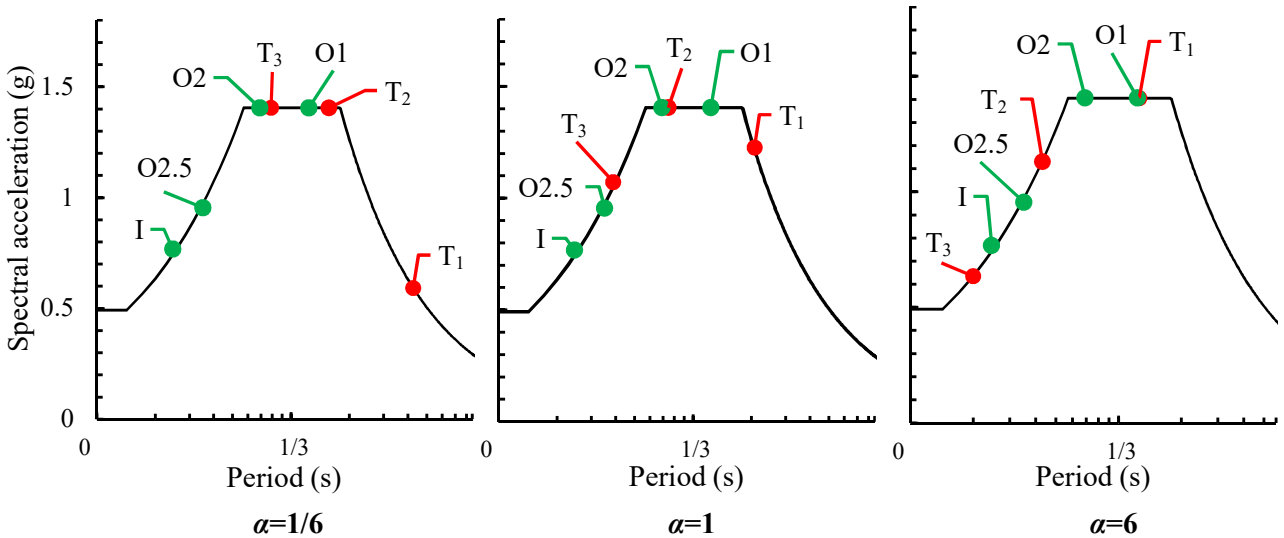

Fig. 7: R_M =4.5: Substructure model and Roof model Periods mapped on the Design Acceleration Spectrum

Table 7: Combined model periods and mode shapes

DL (kPa)	R_M	α	T_1(s) and β (%)	T_2(s) and β (%)	T_3(s) and β (%)
1	11.5	1/6	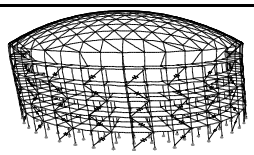 1.2s, (73%)	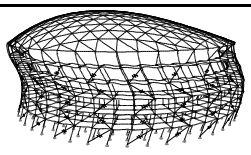 0.5s, (18%)	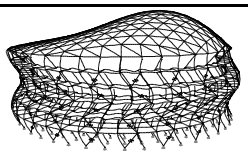 0.2s, (5%)
		1	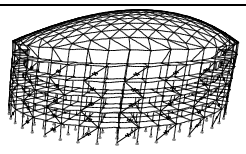 0.5s, (68%)	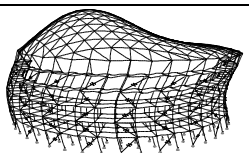 0.2s, (15%)	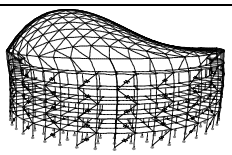 0.3s, (8%)
		6	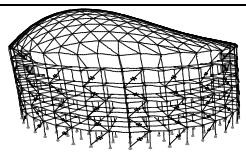 0.3s, (49%)	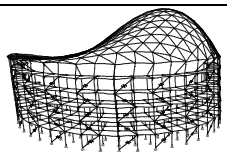 0.2s, (14%)	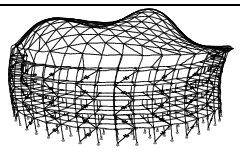 0.1s, (12%)
2	6.2	1/6	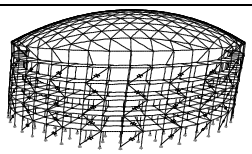 1.3s, (72%)	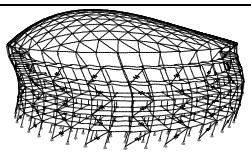 0.5s, (18%)	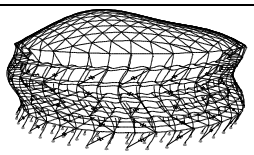 0.3s, (6%)
		1	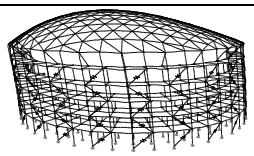 0.6s, (62%)	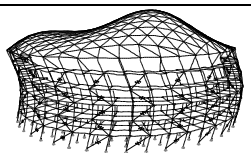 0.2s, (17%)	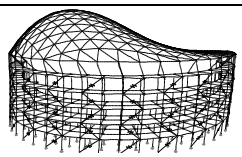 0.4s, (9%)
		6	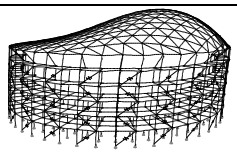 0.4s, (30%)	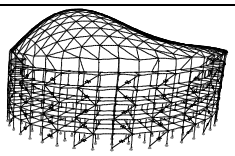 0.3s, (29%)	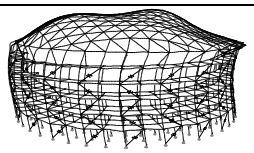 0.1s, (19%)
3	4.5	1/6	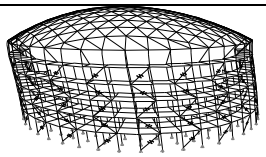 1.5, (71%)	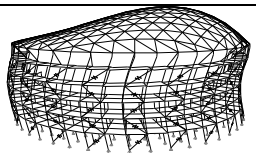 0.6s, (16%)	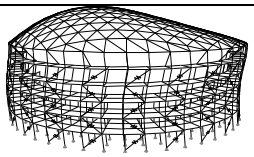 0.5s, (6%)
		1	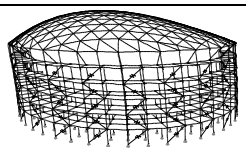 0.7s, (59%)	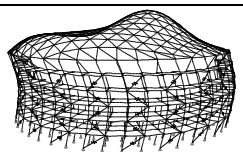 0.3s, (17%)	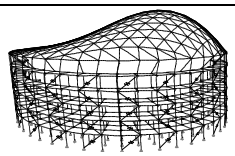 0.5s, (10%)
		6	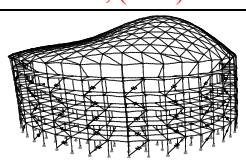 0.4s, (32%)	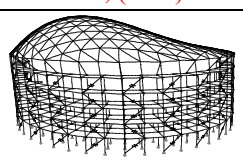 0.5s, (25%)	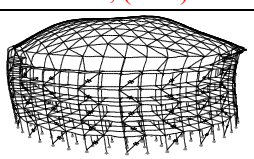 0.2s, (21%)

The periods, mode shapes and the mass participation factors of the first three dominant modes of the corresponding combined models are given in Table 7. The dynamic response characteristics of roofs with soft and flexible substructures (α=1/6) are governed by the translational sway modes of the substructure in combination with the roof's O1 mode. In these cases, the periods and the mass participation factors, therefore, are also similar to the periods obtained from the substructure model. Even though the fundamental periods are longer, the higher modes of the substructure primarily interact with the roof's O1 mode and the higher modes of the roof remain largely unexcited. On the other hand, domes with relatively stiffer substructures (α=1) are governed by several modes with the roof exhibiting O1, O2, O2.5 and I modes in interaction with the translational modes of the substructure with the O1 mode generally being the most dominant. The models with stiffer substructures (α=6) have periods in close proximity to the roof periods and the dominant modes are governed by the interacting roof and substructure modes and hence, the mass participation factors of these modes are also different from those of their substructure models. The seismic response can also be expected to be amplified as a result of resonant effects between the substructure and roof [2].

In addition, mapping the periods of the corresponding substructure models and roof models on the design spectrum (explained later in Section 5) provide an insight into their interactions (Fig.7). Each of the substructure modes can be seen interacting with the nearest roof mode. For example, for the combined model with R_M =4.5 and α=1/6, the first substructure mode is farther apart from the other roof modes and interacts with only the O1 roof mode as shown in Fig. 7. The next dominant mode is the substructure in its second mode interacting with the O1 mode. For α=1, the first substructure mode interacts with the roof's O1 mode. This is followed by the second substructure mode interacting with the nearest roof mode, the O2 mode as both of them have identical periods resulting in its significant mass participation. The third mode is the roof's O1 mode mildly interacting with the substructure's first mode. Similarly, for α=6, the first mode is the first substructure mode interacting with the roof's O1 mode although the mass participation is less than in other cases. The second mode is the roof's O1 mode mildly interacting with the substructure's first mode. The third mode is the substructure's second mode interacting with the nearest roof mode, the O2.5 mode. Thus, the interaction between the roof and substructure is strongly influenced by the relative proximity of the periods of their dominant modes.

5. Response History Analysis Results

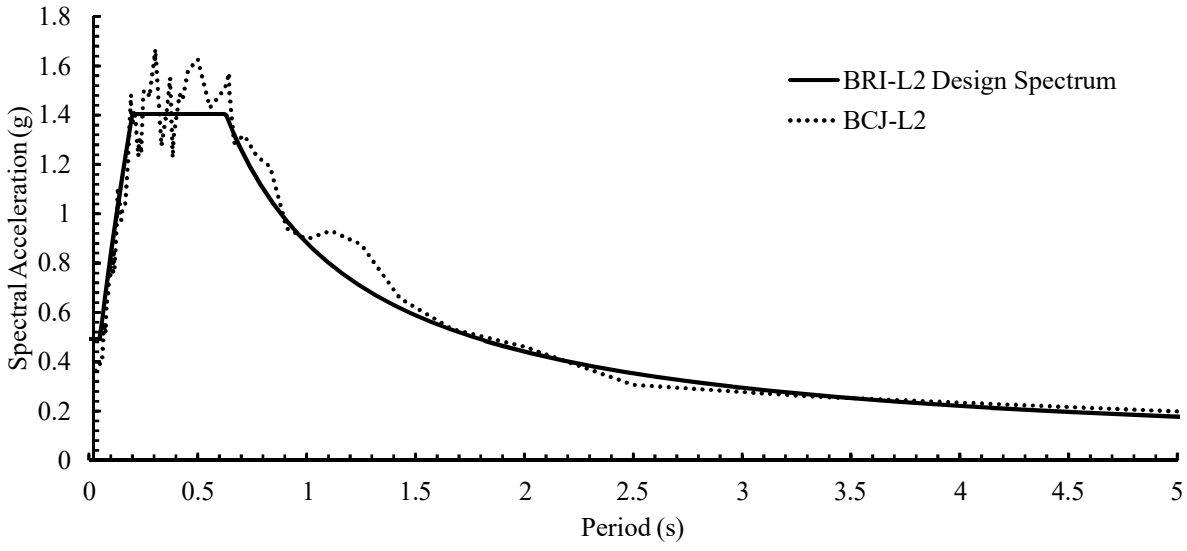

Fig. 8: Level-2 Design Acceleration Spectrum

Linear response history analyses were performed on the combined models subjected to the BCJ-L2 ground motion which is an artificial wave and its response spectrum spectrally matches the level-2 design acceleration spectrum BRI-L2 (Fig. 8) over the entire period range of 0 to 10s. For the analyses, Rayleigh damping of 2% was assigned to the maximum and minimum periods of the first three dominant modes of the structures. The Hilber-Hughes-Taylor (HHT) integration method [6] was used for time-history analyses with computational parameters α equal to 0, β equal to 0.25 and γ equal to 0.5.

Fig. 9 shows the peak horizontal and vertical acceleration distributions along the ridgeline A-O-A'. As observed in the modal analysis results, the horizontal and vertical accelerations are also heavily influenced by the roof-substructure interactions. The horizontal accelerations and the vertical accelerations are amplified more as the substructure becomes stiff as can be seen in Fig 9. For roofs with soft and flexible substructures (α=1/6), the response is governed by the translational sway mode of the substructure and the roof's O1 mode in combination with the second dominant mode of the substructure. On the other hand, domes with slightly stiffer substructures (α=1) are governed by interacting roof and substructure modes with the O1 mode generally being the most dominant except for some of the cases when the substructure's fundamental mode is in the constant velocity (period>0.6s) region (corresponding to a lower acceleration) and the higher mode is in the constant acceleration region (period range = {0.2s, 0.6s}). In such cases, the envelope can be governed by the higher roof mode (R_M=4.5 and α=1). This is similar to the effects observed by Nair et al. [7] where the higher modes of the structure, lying on the constant acceleration region significantly influenced the overall roof response. For models with stiffer substructures (α=6), the roof's response is further amplified as the substructure periods are in the same range as the roof's modes (R_{T1}=1) approaching a state of resonance [2].

$$F_H = \begin{Bmatrix} 3 & (0 < R_T \le 5/16) \\ \sqrt{5/4R_T} & (5/16 < R_T \le 5/4) \\ 1 & (5/4 < R_T) \end{Bmatrix} \quad (1)$$

$$F_V = \begin{Bmatrix} 3C_V\theta & (0 < R_{Ti} \le 5/16) \\ (\sqrt{5/R_T} - 1)C_V\theta & (5/16 < R_T \le 5) \\ 0 & (5 < R_T) \end{Bmatrix} \quad (2)$$

The horizontal and vertical amplification factors, F_H and F_V proposed by Takeuchi et al. [2] which have been adopted in the guide to earthquake response evaluation for metal spatial structures [8] are shown in Eqs. (1) and (2), where θ is the half subtended angle, R_T is the ratio of the fundamental period of the substructure model to that of the roof O1 mode, and the calibration factor C_V is taken as 1.88 [2]. These amplification factors are then multiplied by A_{eq} to obtain the roof accelerations. It is to be noted that the amplification factors were proposed based on the period ratio calculated based on the first mode period of the substructure. These equations indicate that F_V starts to decrease when R_T (defined as R_{T1} in Section 3) becomes larger than 5/16, and approaches 0 as R_T approaches 5 implying that the roof is not excited and the response is primarily governed by the substructure sway modes. In Fig. 9(b), it can be seen that even when R_{T1} is in the range of 4-5 (α=1/6), the vertical accelerations are still amplified and the vertical acceleration distributions do not drop to 0. The distributions here can be explained using the O1 mode of the roof interacting with the higher mode of the substructure. This difference arises because even though R_{T1} is large, the mass participation of the first mode of the multi-storey substructure is less than 80% and the contribution from the higher mode of the substructure becomes significant. In addition, the fundamental periods of these long-span substructures lie on the constant velocity region of the response spectrum but the higher modes lie on the constant acceleration region. Further, for models with relatively stiffer substructures (α=1), the large R_{T1} (~2) values correspond to amplification factors F_V of less than 1, but the peak vertical acceleration responses reflect amplification by larger values which indicates that the contributions and the amplified response based on the substructure's higher modes are significant. Similarly, the amplified horizontal acceleration responses do not reflect F_H of less than 1. Therefore, for domes with longer spans and taller substructures, the amplification factors calculated

based on the higher modes of the substructure need to be included while estimating the seismic response of the roofs which will, in turn, ensure accuracies of the equivalent static loads for the domes calculated based on this response.

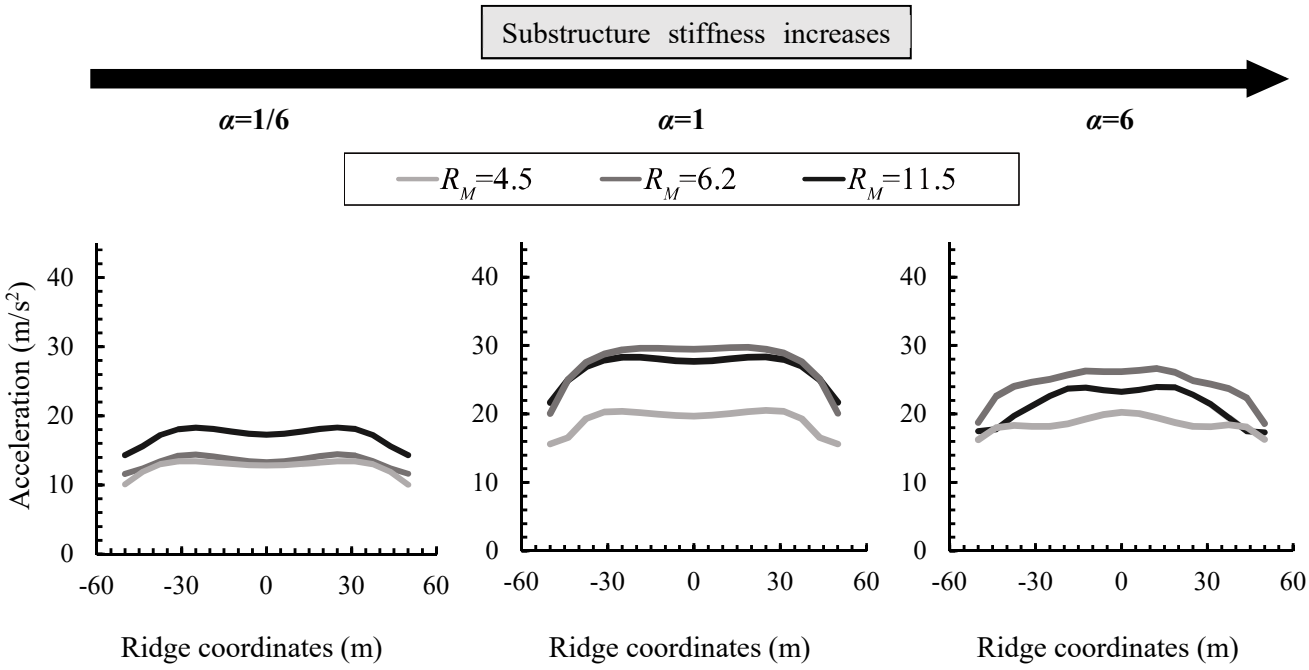

Fig. 9 (a): Horizontal accelerations along the ridgeline

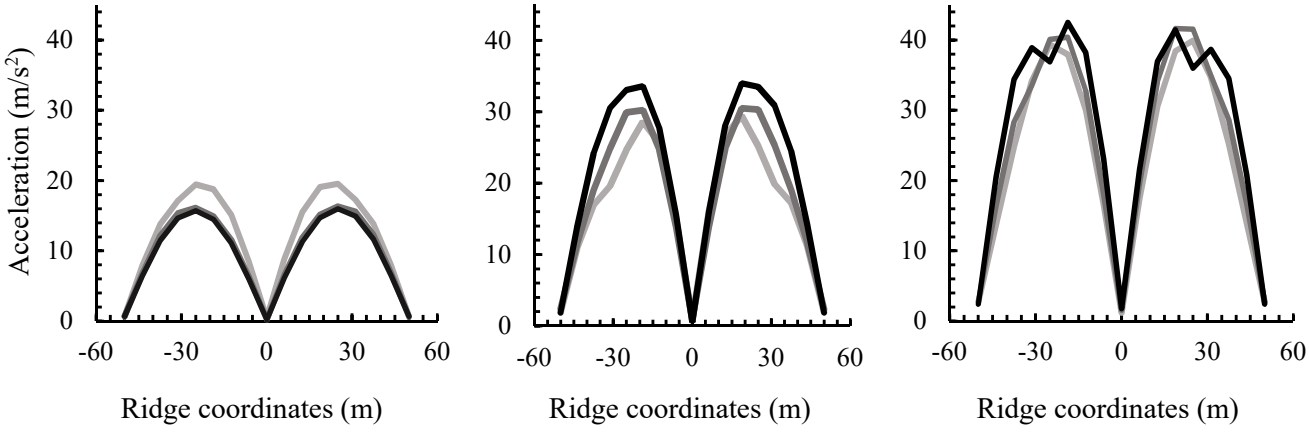

Fig. 9 (b): Vertical accelerations along the ridgeline

6. Conclusions

This paper investigated the dynamic response characteristics of a long-span dome supported by a multi-storey substructure. Effects of mass ratio and substructure stiffness on the periods and mass participation ratios of the dominant modes were examined by conducting a parametric study on a 100m double-layered dome supported by a multi-storey substructure incorporating BRBFs. Following conclusions were drawn from this investigation.

1) The dominant modes of the long-span domes and multi-storey substructures were found to have a direct correlation with the mass ratio, and the effect on the periods was more prominent in the fundamental modes

but the mass participation of these modes largely remained unaffected. The interactions between the roof and substructure in the combined models were strongly influenced by the relative proximity of the periods of the dominant roof and substructure modes.

2) For combined models with multi-storey substructures, the higher modes of the multi-storey substructure and the long-span roof interact with each other resulting in an amplified roof response. This suggests that the previously proposed amplification factors for medium-span domes which are estimated based on the substructure's first mode do not account for the significant amplification arising from these higher mode interactions.
3) For domes with longer spans supported by taller substructures, the peak substructure accelerations and the corresponding roof amplification factors calculated based on the higher modes of the substructure need to be incorporated to accurately estimate the peak seismic response of the roofs.

7. References

[1] T. Ogawa, T. Takeuchi, M. Nakagawa, and T. Kumagai (2003): Seismic response analysis of single-layer lattice domes. *Proceedings of IASS-APCS Symposia*, Taipei, Taiwan.

[2] T. Takeuchi, T. Ogawa, and T. Kumagai (2007): Seismic response evaluation of lattice shell roofs using amplification factors. *Journal of the IASS*, vol. 48, pp. 197–210.

[3] *The Building Standard Law of Japan on CD-ROM* (2016). The Building Center of Japan.

[4] T. Takeuchi and A. Wada (2017): Buckling-Restrained Braces and Applications. JSSI.

[5] T. Takeuchi, T. Kumagai, H. Shirabe, and T. Ogawa (2007): Seismic response evaluation of lattice roofs supported by multistory substructures. *Proceedings of IASS Symposia, Venice, Italy.*

[6] E. L. Wilson (2015): *CSI Analysis Reference Manual for SAP 2000, ETABS, SAFE and CSI Bridge*. Berkeley: Computer & Structures Inc.

[7] D. Nair, Y. Terazawa, B. Sitler, and T. Takeuchi (2019): Seismic Response Evaluation of Long-span Domes Supported by Multi-storey Substructures Incorporating Spine Frames. *Proceedings of IASS Annual Symposia*, Barcelona, Spain.

[8] IASS WG8 for Metal Spatial Structures (2019): *(Draft) Guide to Earthquake Response Evaluation of Metal Roof Spatial Structures.* IASS.

